

Remote Field Eddy Current NDT in Tubes Using Anisotropic Magneto-Resistors

D. J. Pasadas¹, A. Lopes Ribeiro¹, T. J. Rocha¹, H. G. Ramos¹

¹ *Instituto de Telecomunicações, Instituto Superior Técnico, Universidade de Lisboa
Av. Rovisco Pais, 1049-001 Lisboa, Portugal
arturlr@tecnico.ulisboa.pt*

Abstract- This paper presents a measuring system capable of detecting longitudinal and circumferential defects using remote field eddy current in stainless steel tubes with an AMR sensor. An excitation coil is required with a time varying current to produce a magnetic field that penetrates the material on test. The experimental results from both defects are compared with other results for the same material without any defect. The obtained results represent the AMR output magnetic field amplitude and the phase difference between the magnetic field produced by the excitation coil and the magnetic field measured by the AMR sensor. The paper also presents the defect signature for each defect.

I. Introduction

Nowadays non-destructive testing (NDT) plays an important role in the inspection of industry components. The development of computers with good performance, simulation tools, advanced signal processing and new electromagnetic sensors are attracting many scientists to work in the NDT fields. Detection [1], location [2] and characterization [3] of defects are the three basic activities in this field. Eddy current testing (ECT) is an electromagnetic technique of nondestructive testing that allows the inspection of discontinuities in metallic non-ferromagnetic materials. A coil excited with a time-varying current is required to produce a magnetic field that penetrates the component on test. In this article the excitation coil is sinusoidal with constant amplitude. The excitation magnetic field induces currents in the material called eddy currents. The eddy currents are in quasi phase opposition with the excitation current. In the presence of a material defect, the eddy currents are deviated from the defect, changing the current flow and the magnetic field produced by it. This magnetic field is measured with a magnetic detector in order to evaluate the defect's perturbations.

The Remote Field Eddy Current (RFEC) technique is an especial kind of the Eddy Current (EC) technique. It can be applied in tube inspection in order to find defects and wall thickness reductions. A remote field testing (RFT) probe is moved inside the tube to detect internal and external discontinuities with approximately equal sensitivity. The field diffusion along the tube walls is the base of the through-wall indirect technique [4-5]. An excitation coil and a magnetic detector are required, as in the case of classic EC method. The main difference is the relative location of the excitation coil and the detector, as well as the energy paths between them. Small coils are the most used magnetic detector nowadays, but research has recently introduced other magnetic detectors with improved characteristics. The Hall Effect sensor [6] and the magneto-resistors sensor [7] are two detector examples. In this paper, a special attention has been given to the anisotropic magneto-resistors (AMR) from Honeywell, to provide advantages over coil based magnetic sensors. The directional characteristics, high sensitivity with linear response and large bandwidth (DC to 5 MHz) provided by these sensors make them good candidates in the application of defect detection in steel tubes.

II. System Architecture

The inspected material is a sample tube of austenitic stainless steel (AISI 304) with 26 mm of internal diameter and 28 mm of external diameter. This type of steel is non-ferromagnetic and is used in several industries due to its good resistance to corrosion.

The system architecture used in this work is illustrated in Fig. 1. A RFEC probe with an excitation coil and an AMR sensor (HMC 1021Z) from Honeywell, was used to inspect the tube walls. The coil has 131 turns and was excited with a sinusoidal current with constant amplitude by a FLUKE5700A calibrator. The HMC1021Z sensor is configured as a Wheatstone bridge with four magneto-resistive elements. This sensor has one single sensing axis with high sensitivity (1mV/V/gauss) and a field range between ± 6 gauss. The power supply applied to the bridge was 12 V. The AMR sensor signal is preconditioned using an instrumentation amplifier (INA118) with 40 dB of gain.

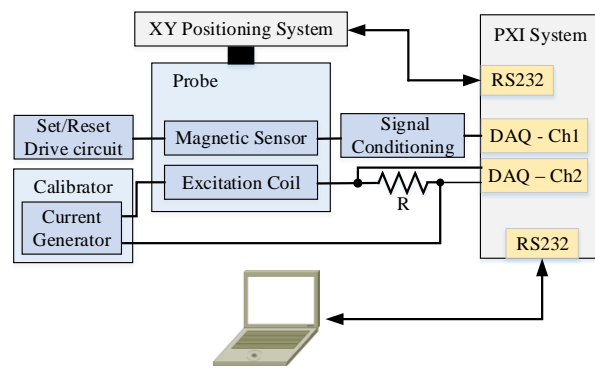


Figure 1. Experimental Setup used in this work.

A set/reset drive circuit providing pulses of electrical current was used to force the sensor to operate in the high sensitivity and linear mode.

A positioning system is used to move the probe along the inner tube wall with steps of 0.5 mm. The positioning system is controlled by a PXI system through a RS232 interface. The PXI system is controlled by the PC with a RS232 interface. A multifunction data acquisition board included in the PXI System is used to measure the AMR sensor output voltage amplified by the instrumentation amplifier and the voltage across the current sampling resistor R. Fig. 2 shows a photograph of the RFEC probe. The excitation coil is placed on the right side and the sensor can be seen 20 mm to the left of the coil. To construct this probe it was necessary to model the complete phenomenon in order to determine the optimum distance between the magnetic sensor and the excitation coil. In the next section a finite element commercial application was used to obtain the magnetic field intensity along the interior tube surface. The AMR field sensor must be placed a certain distance from the coil. Considering the picture in Fig. 2, when the probe is moved along the tube the sensor is always on the left side of the coil. In what follows, as is the case of the experimental results the probe is moved to the right and the sensor is always 20 mm behind the excitation coil.



Figure 2. The RFEC probe photograph.

III. Finite Element Model

Commercial 3D finite element model (FEM) simulation software was used to illustrate the principle of the RFEC technique. To accomplish this task, a simulation was made to obtain the magnetic field along the inner wall of a stainless steel tube (AISI 304), applying an excitation current with 200 mA at 5 kHz. The magnetic permeability of this material is equal to $\mu_0 = 4\pi \times 10^{-7}$ H/m and the electric conductivity is equal to $\sigma = 1.4$ MS/m. Fig. 3 represents the obtained magnetic flux density as a function of the distance between to the excitation coil. From these results it possible to conclude that three zones are visible. One zone directly under the coil, called the direct field zone, a transition zone where the magnetic field decreases sharply, and a third zone where the field intensity decreases exponentially. This last zone is called the remote field zone. In the direct field zone the magnetic flux density produced by the excitation coil dominates, being superimposed by the magnetic field produced by the eddy currents. Hence, this intense magnetic field doesn't allow the detection of the defect in that zone. The magnetic field component that results from the eddy currents diffuses not only across the tube wall thickness, but also longitudinally along the axial direction. Being the eddy currents in an approximately phase opposition with the primary excitation, the resulting field in the transition zone decreases abruptly because these two fields present equal amplitudes.

The primary excitation field is attenuated along the axial direction while the secondary eddy current field continues to diffuse along that direction. Thus, in the remote field zone the field produced by the eddy currents dominates.

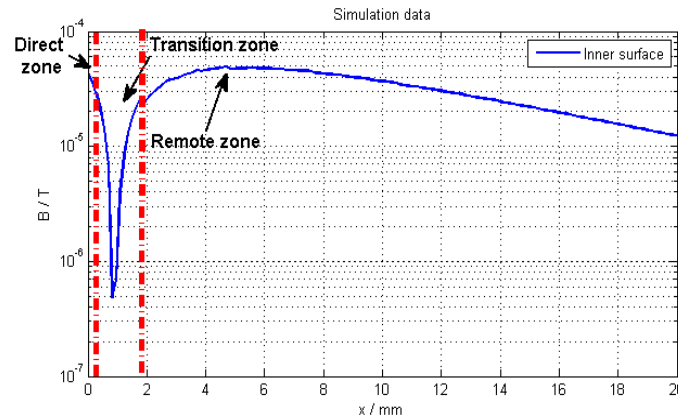


Figure 3. Simulated magnetic field obtained with finite element model.

A transition zone is visible in Fig. 3 that corresponds to the region where the magnetic field produced by the eddy currents begins to overlap the excitation magnetic field and creates a minimum in the magnetic field amplitude due to their opposing phases. The remote zone is the region where the magnetic field produced by eddy current is dominant. Hence, this is the best zone to place the AMR sensor.

IV. Experimental Results

The information obtained in the previous section shows that the distance between the excitation coil and the AMR sensor should be greater than 5 mm to ensure that the measured field is inside the remote zone. In order to ensure that the sensed magnetic field was in the remote zone with minimal attenuation, the chosen distance between the excitation coil and the AMR sensor was 20 mm.

In the experimental results that follow the probe travels from left to right, and the excitation coil goes always ahead. This means that the excitation coil meets a defect before the sensor. The primary excitation field is not affected because the coil excitation current is imposed, but the eddy current under the coil is strongly affected in the case of a longitudinal defect, because this current is circumferential being intersected by the longitudinal defects. This is not the case with circumferential defects that do not intersect most of the eddy currents.

For testing purposes a longitudinal defect and a circumferential defect with both 10 mm length were scanned using the experimental setup. The first experimental test was made by scanning the stainless steel tube (AISI 304), moving the AMR sensor along the inner tube wall without defect in order to obtain the magnetic flux density baseline. The second and third experimental tests were made by scanning an equal tube with a circumferential defect and a longitudinal defect. The applied excitation for all tests was sinusoid with 200 mA of current amplitude at 5 kHz. The AMR output amplitude and the phase difference are represented in Fig. 4 and Fig. 5. The AMR sensing axis was directly along the longitudinal direction, close to the inner tube wall when the magnetic field was measured.

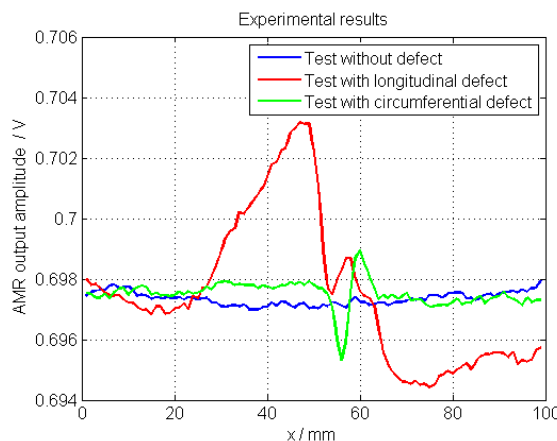


Figure 4. AMR output amplitude in circumferential and longitudinal defect inspection.

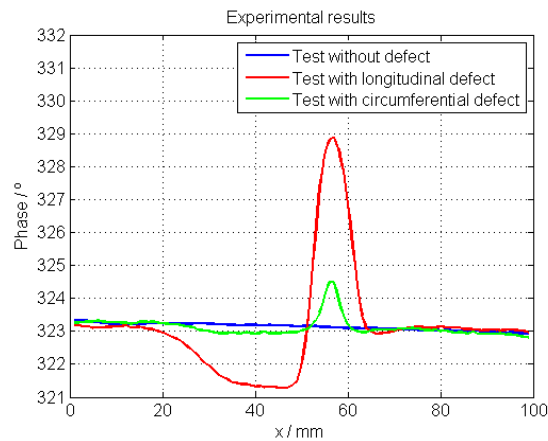


Figure 5. Phase difference obtained in circumferential and longitudinal defect inspection with AMR sensor.

The defect zone is clearly identified by a positive phase peak for each defect in Fig. 5. In the case of the tube sample with longitudinal defect, Fig. 4 and Fig. 5 show an unexpected perturbation before the AMR sensor crosses the defect positions. This is due to the crossing of the excitation coil over the defect, which changes the distribution of the eddy currents in the region under the excitation coil. It also should be noted that the same perturbation with high attenuation was present when the circumferential defect was scanned. In that case, the high attenuation was due to the circumferential nature of the excitation current, the eddy current and the defect itself. To split the two effects, 30 mm were added to the chosen distance between the excitation coil and the AMR sensor in order to ensure that the sensed magnetic field wasn't influenced by the excitation magnetic field variation. The magnetic field measured with this new modification was so small that it was impossible to detect the defect in test. Therefore, the 20 mm of distance between the excitation coil and the AMR sensor continued to be the best option.

Fig. 6 shows the corresponding defect signatures obtained with the experimental amplitude data and the phase difference data in the complex form. These obtained signatures for the two inspected defects show clearly different patterns when compared with the signature obtained for the sample tested without any defect.

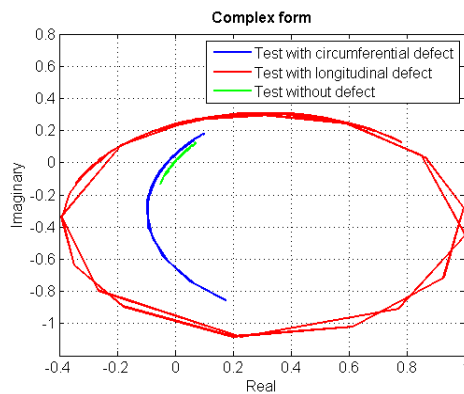


Figure 6. Signatures obtained for the different defect measured.

V. Conclusions

The AMR sensor has shown convincing results for defect detection in stainless steel tubes inspection. This magnetic sensor has directional characteristics and high sensitivity with linear response in a large bandwidth (DC to 5 MHz). The obtained signatures for the two inspected defects show that the AMR sensor is a good option to be implemented in the RFEC instruments.

The chosen distance between the excitation coil and the AMR sensor is important to ensure that the measured field is strong enough to detect defects with minimal signal attenuation.

As future work, improvement of the experimental setup should be made in order to increase the repeatability of the signatures in the defects proximities.

Acknowledgment

This work was developed under the Instituto de Telecomunicações projects KeMANDE and OMEGA and supported in part by the Portuguese Science and Technology Foundation (FCT) projects: PEst-OE/EEI/LA0008/2013, SFRH/BD/81856/2011 and SFRH/BD/81857/2011. This support is gratefully acknowledged.

References

- [1] R. Nagendran, N. Thirumurugan, N. Chinnasamy, M.P. Janawadkar, R. Baskaran, L.S. Vaidhyanathan, C.S. Sundar, "Optimum eddy current excitation frequency for subsurface defect detection in SQUID based non-destructive evaluation", *NDT & E International*, Vol. 43, Issue 8, pp. 713-717, 2010.
- [2] D. Pasadas, T. Rocha, H. G. Ramos, A. L. Ribeiro, "Evaluation of portable ECT instruments with positioning capability", *Measurement*, Vol. 45, No. 1, pp. 393-404, January, 2012.
- [3] A. Bernieri, L. Ferrigno, M. Laracca and M. Molinara, "Crack Shape Reconstruction in Eddy Current Testing Using Machine Learning Systems for Regression", *IEEE Trans. on Instrumentation and Measurement*, Vol. 57, N. 9, pp. 1958–1968, 2008.
- [4] D. L. Atherton and S. Sullivan, "The Remote-Field Through-Wall Electromagnetic Inspection Technique for Pressure Tubes", *Materials Evaluation*, vol. 44, N. 13, pp. 1544–1550, 1986.
- [5] D. L. Atherton and W. Czura, "Finite Element Poynting Vector Calculations for Remote Field Eddy Current Inspection of Tubes with Circumferential Slots", *IEEE Trans. on Magnetics*, vol. 27, N. 5, pp. 3920–3922, 1991.
- [6] Y. He, F. Luo, M. Pan, F. Weng, X. Hu, J. Gao, B.Lui, "Pulse Eddy Current Technique for Defect Detection in Aircraft Riveted Structures", *NDT&E International*, Vol. 43, No. 2, pp. 176-181, Mar.2010.
- [7] A. Jander, C. Smith, R. Schneider, "Magnetoresistive sensors for nondestructive evaluation", Proceedings – SPIE, The Internat. Society For Optimal Engineering, 5770, pp. 1-13, 2005.